An International Journal
JSCDSS
http://www.jscdss.com
Vol.7 No.1 February 2020: 13-18
Article history:
Accepted 06 February 2019
Published online 06February 2019

Journal of Soft Computing and Decision Support Systems

E-ISSN: 2289-8603

Optimum Design of a Dynamic Positioning Controller for an Offshore Vessel

Hamed Ahani [a,*], Milad Familian [b], Reza Ashtari [b]
[a] Mechanical Engineering Department, University of North Carolina at Charlotte, NC, USA, 28262
[b] Electrical Engineering Department, Iran University of Science and Technology, Narmak, Tehran, Iran

*** Corresponding author email address**: hahani@uncc.edu

Abstract

In this paper, an optimal LQG controller is designed to achieve proper dynamic position stabilization on an offshore vessel. The designed control loop operates in the presence of noise from the measurement of sensors, environmental perturbations of waves, winds, and ocean currents. The intended offshore vessel has two side actuators to generate the required torque. The designed controller includes state feedback and an extended Kalman filter. In this study, an additional variable in the system state space is used to improve the performance of the LQG controller in the presence of noise. The results of the simulations performed in the content software show the efficiency of the proposed method compared to the conventional LQG control method. The results of simulations performed in MATLAB reveal a better efficiency of the proposed method compared to the traditional LQG control method.

Keywords: Dynamic position stabilization, Offshore vessel, LQG optimal controller, State feedback, Extended Kalman filter, Ocean current

1. Introduction

Using the issue of dynamic position stabilization (DP) is relevant to the controlling of nonlinear system operators in a surface watercraft for low speed maneuvering or floating maintenance. Operators that produce the control signal on watercraft are generally categorized in two types of propellers and thrusters. Dynamic position stabilization systems have been used commercially on marine watercraft for about 60 years. The mathematical model of the dynamic motion of watercraft, in general, has six degrees of freedom. System modeling based on physical equations along with statistical approaches is conventional methods for constructing an applicable state-space equation for controller design (Golparvar et al., 2016; Modir et al., 2016; Ho et al., 2013; Balchen et al., 1980). Izadi et al (2016) provided a model-based approach combined with the extracted signal from the system to define a realistic mathematical model of an actuator. The extracted model is used not only in the controller design, but also it can be used in applications like fault detection and isolation (Izadi et al., 2017). In the modelling of the offshore vessel for this research, the conventional model based on the physical equation is used. The reason for this approach is the simplicity of the controller design process. In addition, the nonlinearity of the system is not considerably affective on the designed controller performance in the linearized zone (Shahri et al., 2020; Shindgikar et al., 2020; Karimi Shahri et al., 2019; Kelareh et al., 2019; Taremi et al., 2019; Izadi et al., 2017; Izadi et al., 2016; Sørensen, 2011; Fossen & Strand, 1999; Sørensen et al., 1996; Balchen et al., 1976). Especially in (Taremi et al., 2019), the authors investigated an approach to design a tracker by fuzzy polynomial control law. In the proposed method, the nonlinearities of the system are considered. Therefore, the proposed design approach is applicable to a wide range of systems. Floating stabilization is often considered along the x and y axes and the yawing around the z-axis. Hence, most of the studies conducted on stabilizing the dynamic position of the control system have an equation of motion with three degrees of freedom (Ho et al., 2013; Balchen et al., 1980). The first dynamic positioning system uses a PID controller with a series of low-pass and band-stop filters.

Kalman filter theory and optimal control methods have been used to improve the performance of the control system. One of the most commonly used optimal control methods for float position stabilization is the LQG method, which includes an LQR controller and a Kalman filter (Sørensen et al., 1996; Balchen et al., 1976). In general, Kalman filters are used to estimate the state values in the presence of measurement noise and calculating the feedback control gain. For the best performance of this controller, the values of designed gains should be adjusted according to the operating conditions of the offshore vessel. Real-time modification and updating of these gains in the designed controller add complexity to the system and has specific implementation conditions (Fossen & Strand, 1999). In order to detect and remove system noise, different

methods have been used so far. Tabatabai Adnani et al (2016) used Butterworth Low Pass Digital for detecting and removing of the system noise in real simulation (Sørensen, 2011). In this paper, the optimal LQG control method is used to stabilize the dynamic position of the offshore vessel. A new variable has been added to the linearized state space of the system to reduce the complexity of the controller instead of real-time adjustment of LQR gain and Kalman filters. This new variable results from the integral of the difference between the actual and desired output value output. By using this new variable, a modified LQG controller is obtained, which shows better steady-state behavior than the conventional LQG controller. First, the mathematical model of DP is presented, then the design of the proposed LQR controller is discussed. Finally, the numerical results of the heuristic method will be shown with the help of MATLAB.

2. Mathematical Model

There are several mathematical model and formulation that researchers applied to solve the engineering problems (Hosseinzadeh et al., 2019; Mousavisani et al., 2019). Considered Modeling is essential in the design and control of offshore vessels because the model of the ship can be used to evaluate the designs in order to achieve cost reduction. Using a real ship to implement the designed system, the model used the model to conduct initial investigations on the developed model and fix the problems.

In general, a vessel has six degrees of freedom, including linear and rotational motions around its major axes. In the offshore vessels, most movements occur at three degrees of freedom, which are linear motion on the x and *y* axes and the circumference of the *z*-axis. Hence, as shown in Fig. 1, the position, velocity, and force at each degree of freedom are expressed as follows:

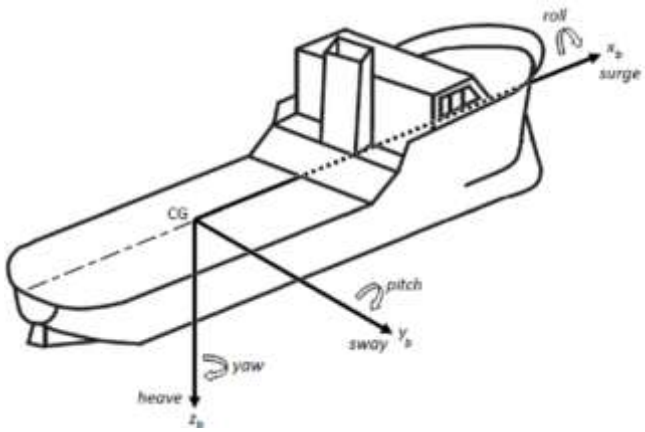

Fig. 1. The coordinates of the offshore vessel.

In vessels, there are often two reference frames or coordinates for small-scale control which include (Sørensen, 2011):

- North-East-Down (NED)
- Body Frame

The reference frame NED, $\{n\} = \{u_n, y_n, z_n\}$ has origin o_n and is assumed to be the tangent plane to the Earth's surface at the desired position from the Earth and inertial frame. In this reference frame, the direction of x_n is oriented to the north, y_n to the east and z_n toward the center of the earth. This reference frame is used for marine vessels which are placed approximately in the same latitude and longitude.

The reference body frame $\{n\} = \{x_n, y_n, z_n\}$ has origin o_n is fixed to a point on the vessel close to the center of gravity. The axis x_n is in the direction of the stern toward the bow, y_n in the direction of the right side and z_n is downward. The velocity vectors *(V)* and force *(τ)* are expressed in the body frame while the position of the vessel is at NED Reference Frame (shown in Fig. 2). The conversion between the inertia frame and the vessel's body on the plane *(x, y)*, in other words, the surge, sway and yaw motion of vessel's body, is expressed as the Eq. (1).

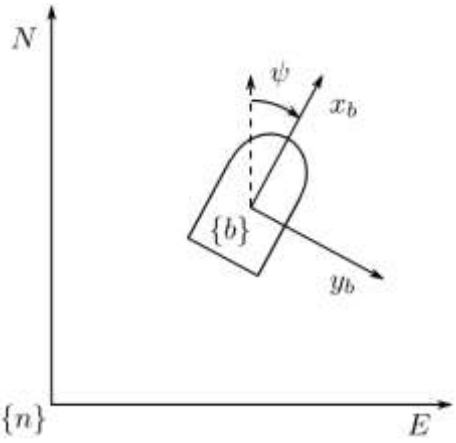

Fig. 2. Body reference in respect to NED reference.

$$R(\psi) = \begin{bmatrix} \cos(\psi) & -\sin(\psi) & 0 \\ \sin(\psi) & \cos(\psi) & 0 \\ 0 & 0 & 1 \end{bmatrix} \quad (1)$$

The yaw angle value is determined by the sensors on the vessel. The acquired data from the sensors on the watercraft generates a rich set for extracting the location and orientation information for the system. Based on the compression methods like (Surakanti et al., 2019), the amount of required storage memory and required bandwidth for communication can be reduced. Therefore, in the provided approach, we supposed that the potential design limitations do not apply any modification on the controller design process. In addition, a conversion matrix is used to indicate the vessel's velocity in the inertial

E-ISSN: 2289-8603

reference frame. Hence, the velocity is defined as the Eq. (2) in the inertial reference:

$$\vec{V}_n = R(\psi)\vec{V}_b \quad (2)$$

In this way, the value of the yaw angle and as the velocity of the vessel at the body frame provides the velocity of the vessel in the inertial reference frame. The equation of motion of the vessel in the inertial frame is expressed as the Eq. (3):

$$M\dot{\vec{V}} + C_{(\vec{v})}\vec{V} + D\vec{V} + d(\vec{V}_r) = \vec{\tau} + \vec{\tau}_d \quad (3)$$

M is inertia matrix, $C_{(\vec{v})}$ Coriolis torque, D shell friction, $d(\vec{V}_r)$ damping torque and $\vec{\tau}_d$ environmental perturbation torque. As stated in the Eq. (4), the ocean currents, waves, and winds are the perturbations torque applied to the body.

$$\vec{\tau}_d = \vec{\tau}_{wind} + \vec{\tau}_{wave} + \vec{\tau}_{current} \quad (4)$$

3. LQG Controller Design

The LQG method is obtained by combining the two LQR problems and the Kalman filter. The system equations in the presence of measurement noise are assumed to be as the Eq. (5) (Welch & Bishop, 2006).

$$\begin{aligned} \dot{x}(t) &= f(x(t),u(t),w(t)) \\ y(t) &= h(x(t),u(t),v(t)) \\ \dot{\vec{v}} &= \vec{M}^{-1}\vec{\tau} - \vec{M}^{-1}\vec{D}\vec{v} \end{aligned} \quad (5)$$

Which $W_{(t)}$ and $v_{(t)}$ are the state noise and the output noise respectively. In order to design the LQG controller for dynamic position stabilization, the floating-point equation is rotated around zero velocity. Using the Taylor series expansion, the system equation is linearized as follows:

On the other hand, since the purpose of the controller design is to stabilize the dynamic position of the vessel, the system equation must also include the position of the system in addition to velocity. Hence, with the above equation the state space is expressed as the Eq. (6):

$$\underbrace{\begin{bmatrix}\dot{\eta}\\ \dot{v}\end{bmatrix}}_{\dot{x}} = \underbrace{\begin{bmatrix}0 & I\\ 0 & M^{-1}D\end{bmatrix}}_{A}\underbrace{\begin{bmatrix}\eta\\ v\end{bmatrix}}_{x} + \underbrace{\begin{bmatrix}0\\ M^{-1}\end{bmatrix}}_{B_u}\underbrace{\tau}_{u} + B_w w$$

$$Y = \eta + D_v \upsilon_n \qquad Z = C_z\begin{bmatrix}\eta\\ v\end{bmatrix} + D_{zu}\tau \quad (6)$$

where the measurement noise and perturbation are considered. B_w is state noise gain, D_v output noise gain and D_{zu}, C_z are input and output gain.

In the LQR case in the LQG controller, the objective is to calculate the state-feedback gain k in order to stabilize the system and minimize the objective cost function. This objective function in the LQR controller is defined as the Eq. (7):

$$J = \int_0^\infty X^T QX + U^T RU\, dt, \quad R = D'_{zu} D_{zu}, \quad Q = C'_z C_z \quad (7)$$

where Q and R are the weight matrix (semi-definite positive) of state vector coefficients and the matrix (positive definite) of the controllers. As shown in the Eq. (8), first the state-feedback gain k is obtained by solving the Riccati differential equation then the value of the input signal U is calculated.

$$\begin{aligned} &PA + A^T P - PBR^{-1}B^T P + Q = 0 \\ &k = -R^{-1}B^T P \\ &u = kx \end{aligned} \quad (8)$$

In the Kalman filter section, the objective of calculating the observer gain F is to minimize the cost function (see the Eq. (9)) and stabilizing the state estimation error.

$$J_f = \int_0^\infty \omega^T Q_n \omega + v^T R_n v\, dt, \quad R_n = D_v D'_v, \quad Q = B_w B'_w \quad (9)$$

The solution of the Riccati equation is used in order to obtain the gain of the observer F. Consequently, the closed-loop equation of the state space will be obtained which is shown in Fig. 3 and is expressed as the Eq. (10):

$$\begin{aligned} &\dot{\hat{x}} = (A + B_u k + FC_y)\hat{x} - Fy, \quad k = -lqr(A,B,Q,R) \\ &u = kx, \qquad\qquad F = -lqr(A',C',Q_n,R_n) \end{aligned} \quad (10)$$

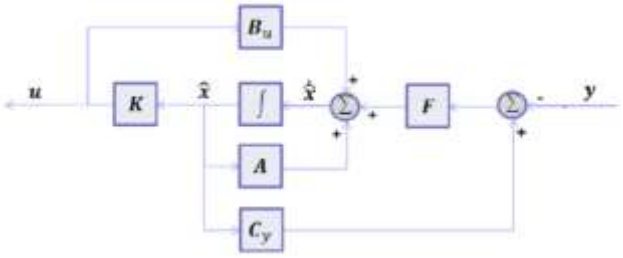

Fig. 3. LQR controller.

Although the designed controller shows a good performance by generating floating-point offset with a nonlinear model. However, by adding perturbation torque of waves to the designed controller system, it generates a permanent error and will not perform suitably as well. In addition to the numerical results as shown in the results section, desired outputs will have steady-state error. Altering the gain in the LQG controller would not solve this problem. Therefore, an integral term is used to omit the steady-state error problem. The source of the perturbation is mostly because of the environmental condition of the watercraft. In this paper, we considered external disturbances like another controller agent, which generates an additional control signal for the system. The used approach to dealing with this situation is based on the

an International Journal JSCDSS E-ISSN: 2289-8603

simplest provided method in (Bagheri et al., 2019: Izadi et al., 2019: Golding, 2005; Welch & Bishop, 2006), which is based on the added integrator in the state variables of the system. It must be considered that the provided method in (Golding, 2005; Welch & Bishop, 2006) is modified for our application. To add an integrator term to the controller, an additional variable is plugged into the equation of state space (see the Eq. (10)). This variable represents the steady-state error value and is the result of the integral of the difference between the output value and the desired position value with a gain. Hence, there is also an adjustment in the equation of state space. The equation of the state space (see the Eq. (11)) in the LQG controller with an integrator is:

$$\begin{bmatrix} \dot{\hat{x}} \\ \dot{\hat{e}} \end{bmatrix} = \begin{bmatrix} (A + B_u k_x + FC_y) & k_e \\ 0 & 0 \end{bmatrix} \begin{bmatrix} \hat{x} \\ \hat{e} \end{bmatrix} + \begin{bmatrix} F \\ I \end{bmatrix} \tau$$
$$\tau = \begin{bmatrix} k_x & k_e \end{bmatrix} \begin{bmatrix} \hat{x} \\ \hat{e} \end{bmatrix} = k_i \begin{bmatrix} \hat{x} \\ \hat{e} \end{bmatrix} \quad (11)$$

The block diagram of this controller is shown in Fig. 4 which K_x, K_e are the gains of error and regulators respectively and defined K_i matrix.

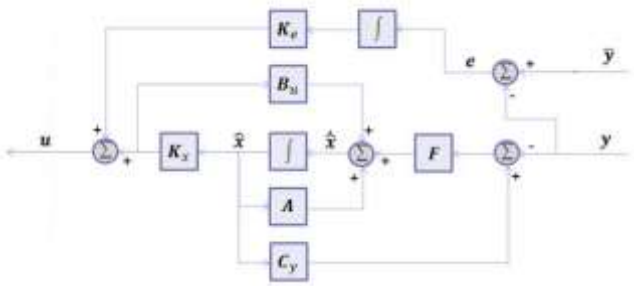

Fig. 4. LQG controller with integrator.

4. Numerical Simulation Results

In this article, the free Naval Control and Navigation Toolbox of the Norwegian University of Science and Technology in MATLAB software were used to implement the designed control methods. The chosen offshore vessel model is CyberShip II. This ship has two-sided thruster and, as shown in Fig. 5, has a lateral and longitudinal distance of 15 and 30 [m] relative to the gravity center of the ship, respectively. First, the nonlinear model of the ship was designed with wind turbulence, ocean waves and currents then the model is linearized. The values of the matrices M and D for the linearized state equation are represented in the Eq. (12).

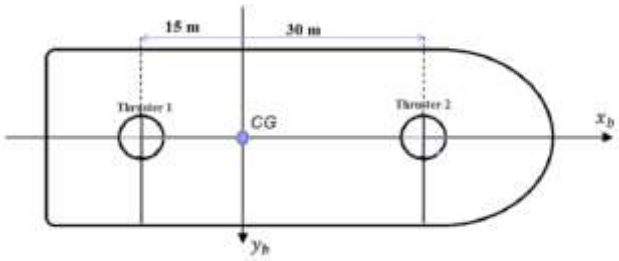

Fig. 5. The position of side Thrusters in the CyberShip II.

$$M = \begin{bmatrix} 25.8 & 0 & 0 \\ 0 & 33.8 & 1.0115 \\ 0 & 1.0115 & 2.76 \end{bmatrix}, D = \begin{bmatrix} 2 & 0 & 0 \\ 0 & 7 & 1 \\ 0 & 1 & 0.5 \end{bmatrix} \quad (12)$$

By applying the obtained linear model obtained, the gain of the LQG and LQG controllers along with the integrator term was obtained (see Eq. (14)). The results of applying this controller to the nonlinear model of the ship with a position offset are shown in Fig. 6, Fig. 7 and Fig. 8 for the x, y, and ψ axes, respectively.

As can be seen, the LQG controller shows good response and in the presence of measurement noise fixes accurately the position of the ship at the reference point $(x,y,\psi)=(0,0,0)$. As shown in Fig. 9, Fig. 10, and Fig. 11, the LQG controller has a steady-state error when the perturbation torque with the velocity of 2 m/s and yaw angle of 30 ° is applied to the ship.

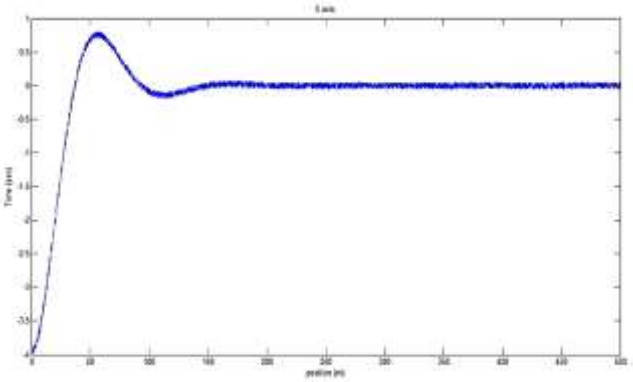

Fig. 6. X-axis status stabilization with LQR controller without perturbation.

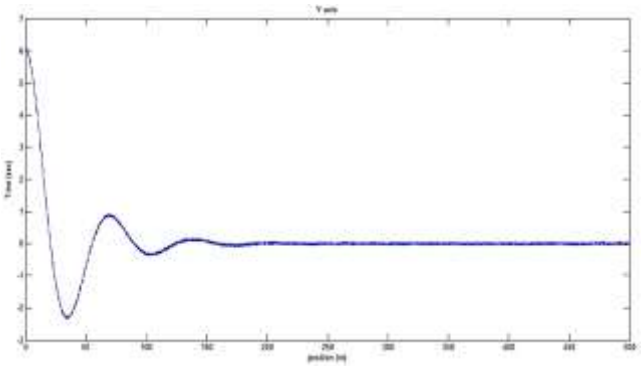

Fig. 7. Y-axis position stabilization with LQR controller without perturbation.

JSCDS
E-ISSN: 2289-8603

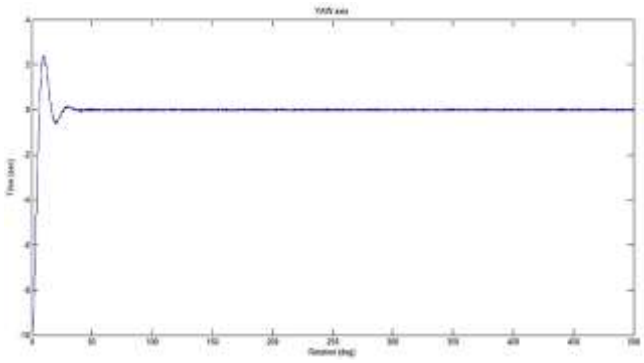

Fig. 8. yaw-axis position stabilization with LQR controller without perturbation.

The steady-state error does not alter significantly with the change of controller gains. However, if the LQG controller is used with the integrator term, the steady-state error will be significantly reduced. This is illustrated in Fig. 12, Fig. 13 and Fig. 14.

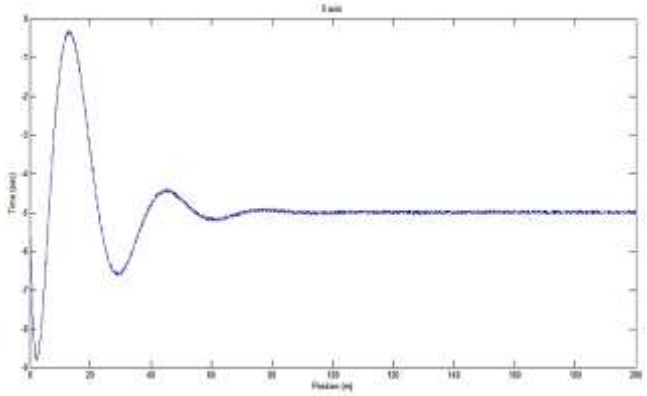

Fig. 9. X-axis position stabilization with LQR controller with perturbation.

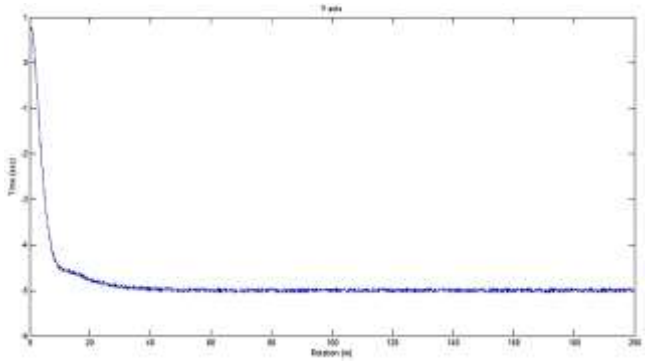

Fig. 10. Y-axis position stabilization with LQR controller with perturbation.

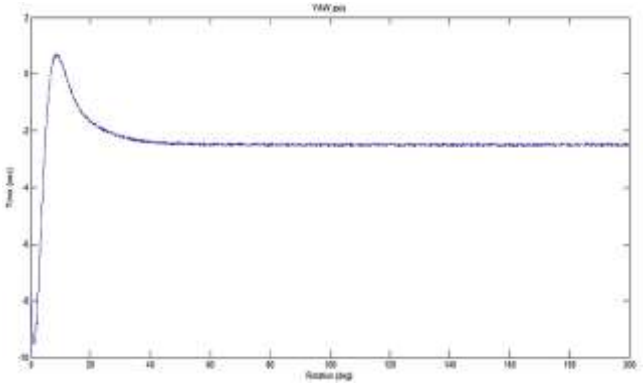

Fig. 11. yaw position stabilization with LQR controller with perturbation.

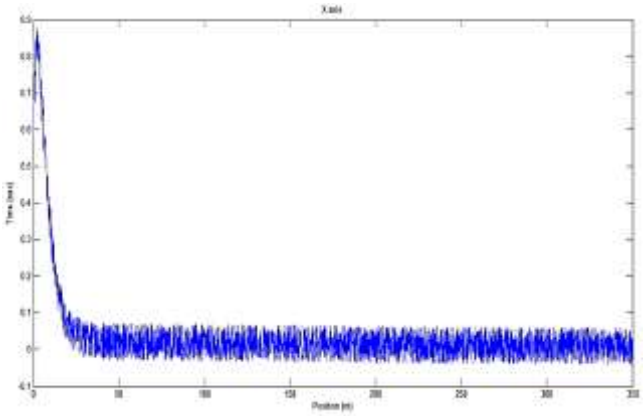

Fig. 12. X-axis position stabilization with LQR controller with integrator and perturbation.

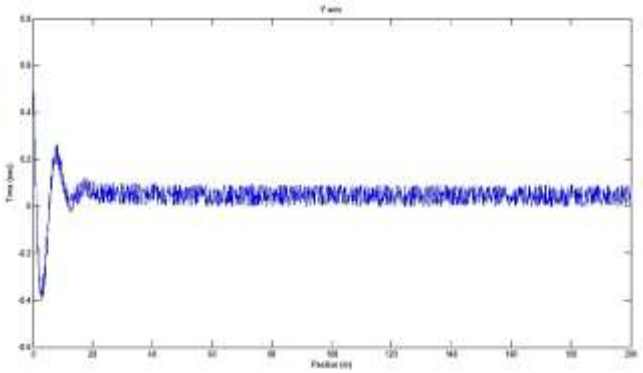

Fig. 13. X-axis position stabilization with LQR controller with integrator and perturbation.

JSCDS
E-ISSN: 2289-8603

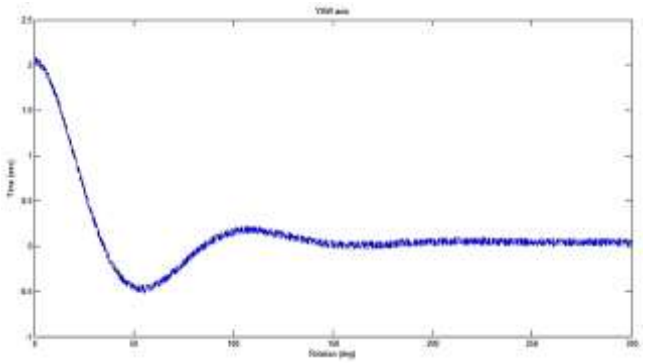

Fig. 14. X-axis position stabilization with LQR controller with integrator and perturbation.

5. Concluding Remark

The In this paper, an optimal LQG controller is designed to stabilize the dynamic position of a scaled model of the ship. The steady-state error problem of this controller was solved by applying a new state variable derived from the error integral. Simulations also showed the effectiveness of the proposed method in the presence of marine perturbations. As a result, this solution can be used to stabilize the position of the offshore vessels.

References

Adnani, A. A. T., Dokami, A., & Morovati, M. (2016). Fault detection in high speed helical gears considering signal processing method in real simulation. Latin American Journal of Solids and Structures, 13(11), 2113-2140.

Bagheri, V., Izadi, V., & Davoodi, K. (2019). Noise-Resistant Feature Extraction from Measured Data of a Passive Sonar. Journal of Soft Computing and Decision Support Systems, 7(1), 1-6.

Balchen, J. G., Jenssen, N. A., & Sælid, S. (1976, September). Dynamic positioning using Kalman filtering and optimal control theory. In IFAC/IFIP symposium on automation in offshore oil field operation (Vol. 183, p. 186).

Balchen, J. G., Jenssen, N. A., Mathisen, E., & Saelid, S. (1980, December). Dynamic positioning of floating vessles based on Kalman filtering and optimal control. In 1980 19th IEEE Conference on Decision and Control including the Symposium on Adaptive Processes (pp. 852-864). IEEE.

Fossen, T. I., & Strand, J. P. (1999). Passive nonlinear observer design for ships using Lyapunov methods: full-scale experiments with a supply vessel. Automatica, 35(1), 3-16.

Golding, B. K. (2005). Modeling and identification of nonlinear viscous drag for ships (Doctoral dissertation, PhD thesis, Norwegian University of Science and Technology).

Golparvar, H., Irani, S., & Sani, M. M. (2016). Experimental investigation of linear and nonlinear aeroelastic behavior of a cropped delta wing with store in low subsonic flow. Journal of the Brazilian Society of Mechanical Sciences and Engineering, 38(4), 1113-1130.

Ho, W. H., Chen, S. H., & Chou, J. H. (2013). Optimal control of Takagi–Sugeno fuzzy-model-based systems representing dynamic ship positioning systems. Applied Soft Computing, 13(7), 3197-3210.

Hosseinzadeh, K., Asadi, A., Mogharrebi, A. R., Khalesi, J., Mousavisani, S., & Ganji, D. D. (2019). Entropy generation analysis of (CH2OH) 2 containing CNTs nanofluid flow under effect of MHD and thermal radiation. Case Studies in Thermal Engineering, 14, 100482.

Hosseinzadeh, K., Mogharrebi, A. R., Asadi, A., Sheikhshahrokhdehkordi, M., Mousavisani, S., & Ganji, D. D. (2019). Entropy generation analysis of mixture nanofluid (H2O/c2H6O2)–Fe3O4 flow between two stretching rotating disks under the effect of MHD and nonlinear thermal radiation. International Journal of Ambient Energy, 1-13.

Izadi, V., Yeravdekar, A., & Ghasemi, A. (2019, November). Determination of roles and interaction modes in a haptic shared control framework. In ASME 2019 Dynamic Systems and Control Conference. American Society of Mechanical Engineers Digital Collection.

Izadi, V., Abedi, M., & Bolandi, H. (2017). Supervisory algorithm based on reaction wheel modelling and spectrum analysis for detection and classification of electromechanical faults. IET Science, Measurement & Technology, 11(8), 1085-1093.

Izadi, V., Abedi, M., & Bolandi, H. (2016, January). Verification of reaction wheel functional model in HIL test-bed. In 2016 4th International Conference on Control, Instrumentation, and Automation (ICCIA) (pp. 155-160). IEEE.

Karimi Shahri, P., Chintamani Shindgikar, S., HomChaudhuri, B., & Ghasemi, A. H. Optimal Lane Management in Heterogeneous Traffic Network. In ASME 2019 Dynamic Systems and Control Conference. American Society of Mechanical Engineers Digital Collection.

Kelareh, A. Y., Shahri, P. K., Khoshnevis, S. A., Valikhani, A., & Shindgikar, S. C. (2019). Dynamic Specification Determination using System Response Processing and Hilbert-Huang Transform Method. International Journal of Applied Engineering Research, 14(22), 4188-4193.

Lv, C., Zhang, J., & Li, Y. (2014). Extended-Kalman-filter-based regenerative and friction blended braking control for electric vehicle equipped with axle motor considering damping and elastic properties of electric powertrain. Vehicle System Dynamics, 52(11), 1372-1388.

Modir, A., Kahrom, M., & Farshidianfar, A. (2016). Mass ratio effect on vortex induced vibration of a flexibly mounted circular cylinder, an experimental study. International journal of marine energy, 16, 1-11.

Shahri, P. K., Ghasemi, A. H., & Izadi, V. (2020). Traffic Control Strategies for Congested Heterogeneous Multi-Vehicle Networks (No. 2020-01-0086). SAE Technical Paper.

Shindgikar, S. C., Shahri, P. K., & Ghasemi, A. H. (2020). Optimal Traffic Management In Urban Traffic Network Using PTV VISSIM And MATLAB SIMULINK (No. 2020-01-0887). SAE Technical Paper.

Sørensen, A. J., Leira, B., Peter Strand, J., & Larsen, C. M. (2001). Optimal setpoint chasing in dynamic positioning of deep-water drilling and intervention vessels. International Journal of Robust and Nonlinear Control: IFAC-Affiliated Journal, 11(13), 1187-1205.

Sørensen, A. J. (2011). A survey of dynamic positioning control systems. Annual reviews in control, 35(1), 123-136.

Surakanti, S. R., Khoshnevis, S. A., Ahani, H., & Izadi, V. (2019). Efficient Recovery of Structrual Health Monitoring Signal based on Kronecker Compressive Sensing. International Journal of Applied Engineering Research, 14(23), 4256-4261.

Taremi, R. S., Shahri, P. K., & Kalareh, A. Y. (2019). Design a Tracking Control Law for the Nonlinear Continuous Time Fuzzy Polynomial Systems. Journal of Soft Computing and Decision Support Systems, 6(6), 21-27.

Welch, G., & Bishop, G. (2006). *An introduction to the Kalman filter, UNC-Chapel Hill* (p. 16). TR 95-041.

E-ISSN: 2289-8603